A non-slip boundary condition
for lattice Boltzmann simulations

Takaji Inamuro, Masato Yoshino, and Fumimaru Ogino

Department of Chemical Engineering, Kyoto University, Kyoto 606-01, Japan

A non-slip boundary condition at a wall for the lattice Boltzmann method is presented. In the present method unknown distribution functions at the wall are assumed to be an equilibrium distribution function with a counter slip velocity which is determined so that fluid velocity at the wall is equal to the wall velocity. Poiseuille flow and Couette flow are calculated with the nine-velocity model to demonstrate the accuracy of the present boundary condition.

1

Recently, the lattice Boltzmann (LB) method[1−4] has been used for many kinds of simulations of viscous flows. In particular, the LB method has been successfully applied to problems of fluid flows through porous media[5,6] and multiphase fluid flows.[7,8] On the other hand, as for the implementation of a non-slip boundary condition several approaches have been proposed.[9−14] The bounce-back boundary condition[9] has been usually used to model stationary walls. However, it has been found that the bounce-back boundary condition has errors in velocity at the wall.[11−14] Skordos[10] proposed a method for calculating particle distributions at a boundary node from fluid variables with the gradients of the fluid velocity. In his method the density is assumed to be known at the boundary. Noble *et al.*[11] developed a method for calculating the density at the boundary and the unknown components of the particle distributions. While their method gives accurate results with the seven-velocity model, it is not clear whether the method can be applied to other velocity models.

In this Letter, a new approach for applying the non-slip boundary condition at the wall is presented. For explanation we use the LB method with the BGK collision model.[3,4] In the method the evolution of the distribution function $f_i(\mathbf{x}, t)$ of particles with velocity $\mathbf{c}_i$ at the point $\mathbf{x}$ and at time t is computed by the following equation:

$$f_i(\mathbf{x} + \mathbf{c}_i \Delta t, t + \Delta t) - f_i(\mathbf{x}, t) = -\frac{1}{\tau}[f_i(\mathbf{x}, t) - f_i^{\mathrm{eq}}(\mathbf{x}, t)], \qquad (1)$$

where $f_i^{\mathrm{eq}}(\mathbf{x}, t)$ is an equilibrium distribution function, τ is a single relaxation time, and Δt is a time step during which the particles travel a grid spacing. The fluid mass density ρ and the fluid velocity $\mathbf{u}$ are defined in terms of the particle distribution function by

$$\rho = \sum_i f_i, \qquad (2)$$

$$\mathbf{u} = \frac{1}{\rho} \sum_i f_i \mathbf{c}_i. \qquad (3)$$

Here, we use the nine-velocity model[4,15] to explain the procedure of the method, but it is straight-forward to apply the method to other velocity models. The nine-velocity model has velocity vectors, $\mathbf{c}_0 = \mathbf{0}$, $\mathbf{c}_i^I = [\cos(\pi(i-1)/2), \sin(\pi(i-1)/2)]$, and $\mathbf{c}_i^{II} = \sqrt{2}[\cos(\pi(i-\frac{1}{2})/2), \sin(\pi(i-\frac{1}{2})/2)]$

for $i = 1, \cdots, 4$. An equilibrium distribution function of this model is given by

$$f_0^{\text{eq}} = \frac{4}{9}\rho(1 - \frac{3}{2}\mathbf{u}^2), \tag{4}$$

$$f_i^{I,\text{eq}} = \frac{\rho}{9}\left[1 + 3(\mathbf{c}_i^I \cdot \mathbf{u}) + \frac{9}{2}(\mathbf{c}_i^I \cdot \mathbf{u})^2 - \frac{3}{2}\mathbf{u}^2\right], \tag{5}$$

$$f_i^{II,\text{eq}} = \frac{\rho}{36}\left[1 + 3(\mathbf{c}_i^{II} \cdot \mathbf{u}) + \frac{9}{2}(\mathbf{c}_i^{II} \cdot \mathbf{u})^2 - \frac{3}{2}\mathbf{u}^2\right]. \tag{6}$$

At the non-slip wall we must specify the distribution functions of the particles whose velocity points to fluid region. In Fig. 1 the distribution functions f_2^I, f_1^{II}, and f_2^{II} are unknowns. In the kinetic theory of gases the assumption of diffuse reflection is often used at the wall. In this approximation gas molecules that strike the wall are assumed to leave it with a Maxwellian velocity distribution having the velocity and the temperature of the wall. In general, the velocity along the wall obtained with this assumption is not equal to that of the wall velocity, although the normal velocity to the wall is equal to that of the wall velocity. The difference between the fictitious velocity and the wall velocity is called the slip velocity. The idea of the present method is that the unknown distribution functions are assumed to be an equilibrium distribution function with a counter slip velocity which is determined so that the fluid velocity at the wall is equal to the wall velocity. That is, in the case of Fig. 1 the unknown distribution functions f_2^I, f_1^{II}, and f_2^{II} are assumed to be

$$f_2^I = \frac{1}{9}\rho'\left[1 + 3v_{\text{w}} + \frac{9}{2}v_{\text{w}}^2 - \frac{3}{2}[(u_{\text{w}} + u')^2 + v_{\text{w}}^2]\right], \tag{7}$$

$$f_1^{II} = \frac{1}{36}\rho'\left[1 + 3(u_{\text{w}} + u' + v_{\text{w}}) + \frac{9}{2}(u_{\text{w}} + u' + v_{\text{w}})^2\right.$$
$$\left. - \frac{3}{2}[(u_{\text{w}} + u')^2 + v_{\text{w}}^2]\right], \tag{8}$$

$$f_2^{II} = \frac{1}{36}\rho'\left[1 + 3(-u_{\text{w}} - u' + v_{\text{w}}) + \frac{9}{2}(-u_{\text{w}} - u' + v_{\text{w}})^2\right.$$
$$\left. - \frac{3}{2}[(u_{\text{w}} + u')^2 + v_{\text{w}}^2]\right], \tag{9}$$

where u_{w} and v_{w} are the x and y components of the wall velocity, and ρ' and u' are unknown parameters. The unknown u' is the above-mentioned counter slip velocity. It is noted that we have no normal velocity jump at the wall because as mentioned above there exists no difference of the normal velocity to the wall between the fluid and the wall on the assumption of diffuse

reflection. The two unknown parameters are determined on the condition that the fluid velocity at the wall is equal to the wall velocity. Thus, we obtain two equations corresponding to the x and y components of the fluid velocity. Moreover, the density at the wall, ρ_{w}, is an unknown quantity and is calculated by Eq. (2). Therefore, we finally obtain three equations for the three unknowns. The solutions are as follows:

$$\rho_{\mathrm{w}} = \frac{1}{1 - v_{\mathrm{w}}}\left[f_0 + f_1^I + f_3^I + 2(f_4^I + f_3^{II} + f_4^{II})\right], \tag{10}$$

$$\rho' = 6\frac{\rho_{\mathrm{w}}v_{\mathrm{w}} + (f_4^I + f_3^{II} + f_4^{II})}{1 + 3v_{\mathrm{w}} + 3v_{\mathrm{w}}^2}, \tag{11}$$

$$u' = \frac{1}{1 + 3v_{\mathrm{w}}}\left[6\frac{\rho_{\mathrm{w}}u_{\mathrm{w}} - (f_1^I - f_3^I + f_4^{II} - f_3^{II})}{\rho'}\right.$$

$$\left. -u_{\mathrm{w}} - 3u_{\mathrm{w}}v_{\mathrm{w}}\right]. \tag{12}$$

It is noted that the same procedure can be applied to other velocity models in spite of the number of particle velocities. In general, for isothermal models in D-dimensional space we have D+1 constraints (D equations for each component of the velocity and one density equation at the wall) for D unknown parameters (ρ' and D−1 slip velocities) and an unknown density at the wall.

To demonstrate the accuracy of the present boundary condition, Poiseuille flow is calculated with the nine-velocity model. A two-dimensional steady flow between stationary parallel walls at $y = -L$ and $y = +L$ with a constant pressure gradient is considered. The pressure gradient is maintained by a density difference between inlet and outlet. At the inlet and the outlet the unknown distribution functions are determined as follows.[16] At the inlet, the unknown distribution functions f_1^I, f_1^{II}, and f_4^{II} are calculated by adding a constant value to the corresponding distribution functions at the outlet so that $f_1^I|_{\mathrm{in}} = f_1^I|_{\mathrm{out}} + C$, $f_1^{II}|_{\mathrm{in}} = f_1^{II}|_{\mathrm{out}} + \frac{1}{4}C$, and $f_4^{II}|_{\mathrm{in}} = f_4^{II}|_{\mathrm{out}} + \frac{1}{4}C$ with reference to the equilibrium distribution functions given by Eqs. (5) and (6). The constant value C is determined by setting the density calculated by Eq. (2) to be a given value at the inlet. The same procedure is used for calculating the unknown distribution functions at the outlet. In addition, the unknown distribution functions at four corners of the inlet and the outlet are calculated as follows. For example, at the lower corner of inlet, f_1^I and

f_4^{II} are calculated by the above-mentioned method. Then, f_2^I, f_1^{II}, and f_2^{II} are calculated by the present non-slip boundary condition. The same method is used at the other three corners. In the following calculations 21 nodes are used between the walls. Figure 2 shows calculated velocity profiles $u/u_{\max}$ ($u_{\max}$ is the velocity at $y = 0$) with the present boundary condition for various values of τ. It is found that the results for $0.7 \leq \tau \leq 20$ agree with the analytical solution within machine accuracy. The values of the counter slip velocity u' are shown in Fig. 3. It is noted that the values of u' are negative for all τ. The magnitude of the counter slip velocity increases as τ becomes larger. Needless to mention, the magnitude of the counter slip velocity depends on the number of nodes between the walls. For comparison with the present results, the results with the bounce-back boundary condition in which $f_2^I = f_4^I, f_1^{II} = f_3^{II}$, and $f_2^{II} = f_4^{II}$ are shown in Fig. 4. Also, the results under the condition with $u' = 0$ in the present boundary condition, which corresponds to the usual diffuse reflection in the kinetic theory of gases, are shown in Fig. 5. It is seen that both results in Fig. 4 and Fig. 5 have slip velocities at the wall and the slip velocity increases as τ becomes larger. In addition, we can see that the slip velocity under the condition with $u' = 0$ in the present boundary condition is larger than that with the bounce-back boundary condition for the same value of τ. This is because the bounce-back boundary condition has stronger non-slip effect than the usual diffuse reflection. In the next problem, we calculate Couette flow to demonstrate the accuracy of the LB method with the present boundary condition. In the problem, the upper plate at $y = +L$ is moved with velocity U at $t > 0$, and the lower plate at $y = -L$ is at rest. Figure 6 shows the calculated velocity profiles u/U at 200 time steps with 21 nodes between the walls and with $\tau = 1$. It is seen that the results agree well with the analytical solution. To determine the convergence rate, we perform simulations with 11, 21, 41, and 81 nodes between the walls. The errors are compared at the same dimensionless time corresponding to 200 time steps with 21 nodes. Figure 7 shows the error norms $E_1 = \sum_y |u - u^*| / \sum_y |u^*|$ and $E_2 = \sqrt{\sum_y (u - u^*)^2} / \sqrt{\sum_y (u^*)^2}$ where u^* is the analytical solution and the sums are taken over the same internal 9 nodes between the walls for all cases. The slope, m, of the convergence is $m = 2.0004$ for E_1, and $m = 2.0006$ for E_2. It is clearly found that the LB method with the present boundary condition is a second-order

scheme.

From these results, we can conclude that the present boundary condition is accurate to model a non-slip flat boundary in the lattice Boltzmann simulations. It should be noted, however, that the present method has difficulties in dealing with corners. One of the possible ways to handle corners is to calculate the unknown distribution functions on each side at the corner and to average the results of common unknown distribution functions, while we should keep in mind that this approach produces errors due to rounded corners. More rigorous considerations for corners remain in future work. Although we use the nine-velocity model to explain the present boundary condition, the method can be directly applied to other velocity models; even to thermal models and to three-dimensional models. For thermal models, we may use an equilibrium distribution function with a counter temperature jump as well as the counter slip velocity. The value of the counter temperature jump can be determined by the condition for temperature at the wall. For three-dimensional models, we may use a counter slip velocity which has two components on the surface of the wall. The calculated results with the other velocity models will be reported in the future.

[1] G. McNamara, and G. Zanetti, "Use of the Boltzmann equation to simulate lattice-gas automata," Phys. Rev. Lett. **61**, 2332 (1988).

[2] F. Higuera and J. Jimenez, "Boltzmann approach to lattice gas simulations," Europhys. Lett. **9**, 663 (1989).

[3] S. Chen, H. Chen, D. Martinez, and W.H. Matthaeus, "Lattice Boltzmann model for simulation of magnetohydrodynamics," Phys. Rev. Lett. **67**, 3776 (1991).

[4] Y.H. Qian, D. d'Humières, and P. Lallemand, "Lattice BGK models for Navier-Stokes equation," Europhys. Lett. **17**, 479 (1992).

[5] S. Succi, E. Foti, and F. Higuera, "Three-dimensional flows in complex geometries with the lattice Boltzmann method," Europhys. Lett. **10**, 433 (1989).

[6] A. Cancelliere, C. Chang, E. Foti, D.H. Rothman, and S. Succi, "The permeability of a random medium: comparison of simulation with theory," Phys. Fluids A **2**, 2085 (1990).

[7] A.K. Gunstensen, D.H. Rothman, and S. Zaleski, "Lattice Boltzmann model of immiscible fluids," Phys. Rev. A **43**, 4320 (1991).

[8] D. Grunau, S. Chen, and K. Eggert, "A lattice Boltzmann model for multiphase fluids flows," Phys. Fluids A **5**, 2557 (1993)

[9] D. d'Humières and P. Lallemand, "Numerical simulations of hydrodynamics with lattice gas automata in two dimensions," Complex Syst. **1**, 599 (1987).

[10] P.A. Skordos, "Initial and boundary conditions for the lattice Boltzmann method," Phys. Rev. E **48**, 4823 (1993).

[11] D.R. Noble, S. Chen, J.G. Georgiadis, and R.O. Buckius, "A consistent hydrodynamic boundary condition for the lattice Boltzmann method," Phys. Fluids **7**, 203 (1995).

[12] R. Cornubert, D. d'Humières, and D. Levermore, "A Knudsen layer theory for lattice gases," Physica D **47**, 241 (1991).

[13] D.P. Ziegler, "Boundary conditions for lattice Boltzmann simulations," J. Stat. Phys. **71**, 1171 (1993).

[14] I. Ginzbourg and P.M. Adler, "Boundary flow condition analysis for the three-dimensional lattice Boltzmann model," J. Phys. II France **4**, 191 (1994).

[15] B.T. Nadiga, "A Study of Multi-Speed Discrete-Velocity Gases," Ph. D Thesis, California Institute of Technology, 1992.

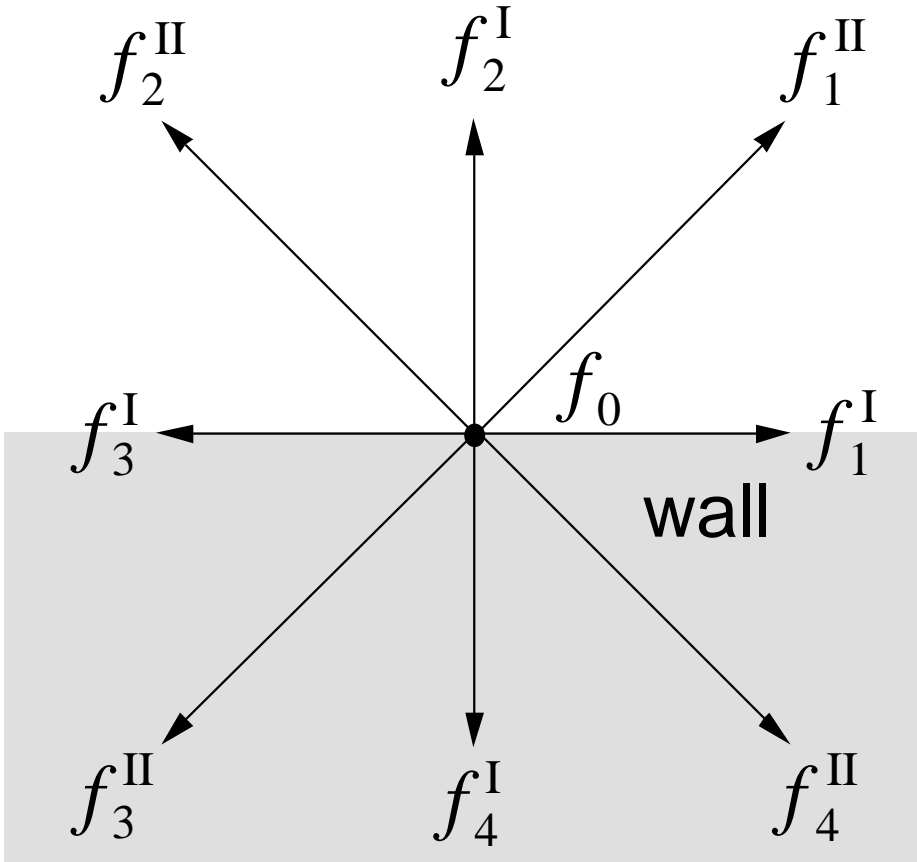[16] T. Inamuro, M. Yoshino, and F. Ogino, in preparation.

FIGURE CAPTION

Fig. 1. Particle distribution functions of the nine-velocity model at the wall.

Fig. 2. Calculated velocity profiles for Poiseuille flow with the present boundary condition for various values of τ.

Fig. 3. Counter slip velocity u' versus single relaxation time τ in the calculations with the present boundary condition.

Fig. 4. Calculated velocity profiles for Poiseuille flow with the bounce-back boundary condition for various values of τ.

Fig. 5. Calculated velocity profiles for Poiseuille flow under the condition with $u' = 0$ in the present boundary condition for various values of τ.

Fig. 6. Calculated velocity profiles for Couette flow at 200 time steps with 21 nodes between the walls and with $\tau = 1$.

Fig. 7. Error norms for Couette flow calculations with 11, 21, 41, and 81 nodes between the walls.

Fig. 1. Particle distribution functions of the nine-
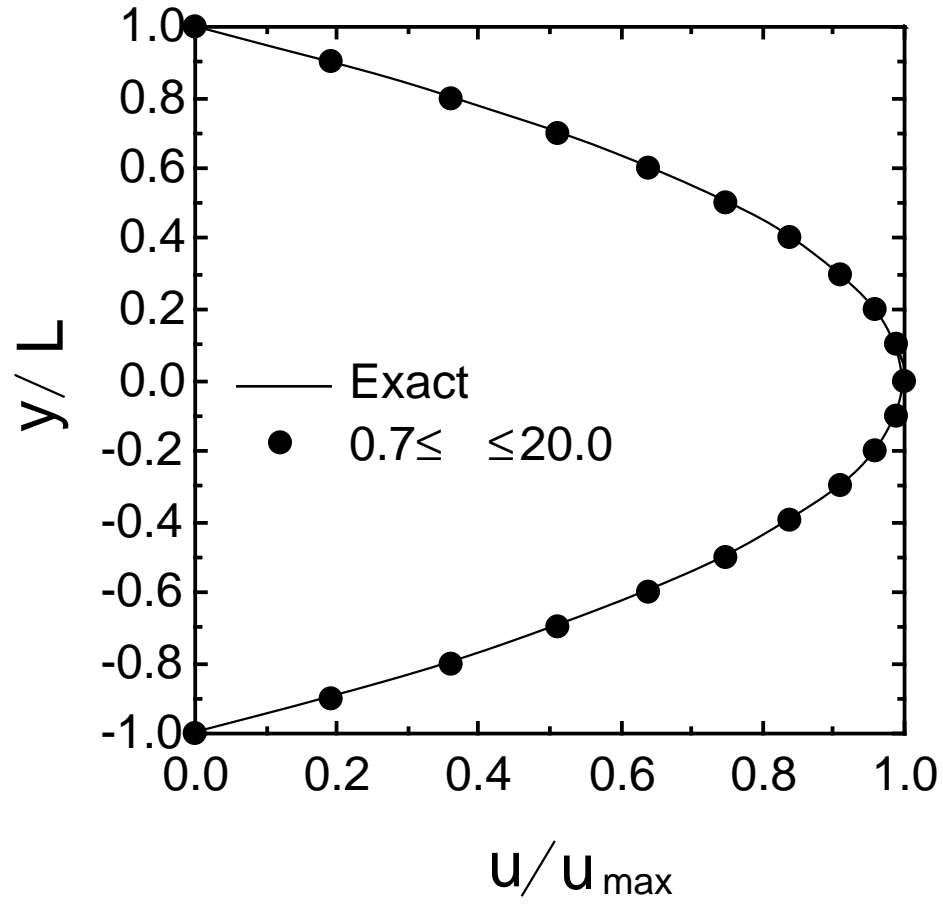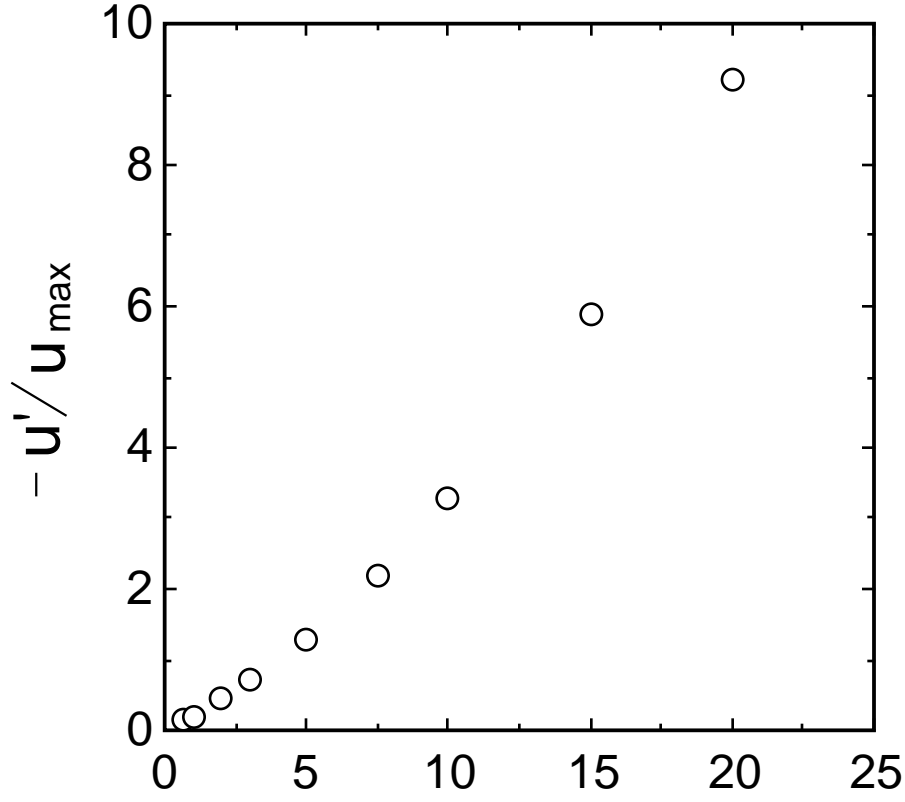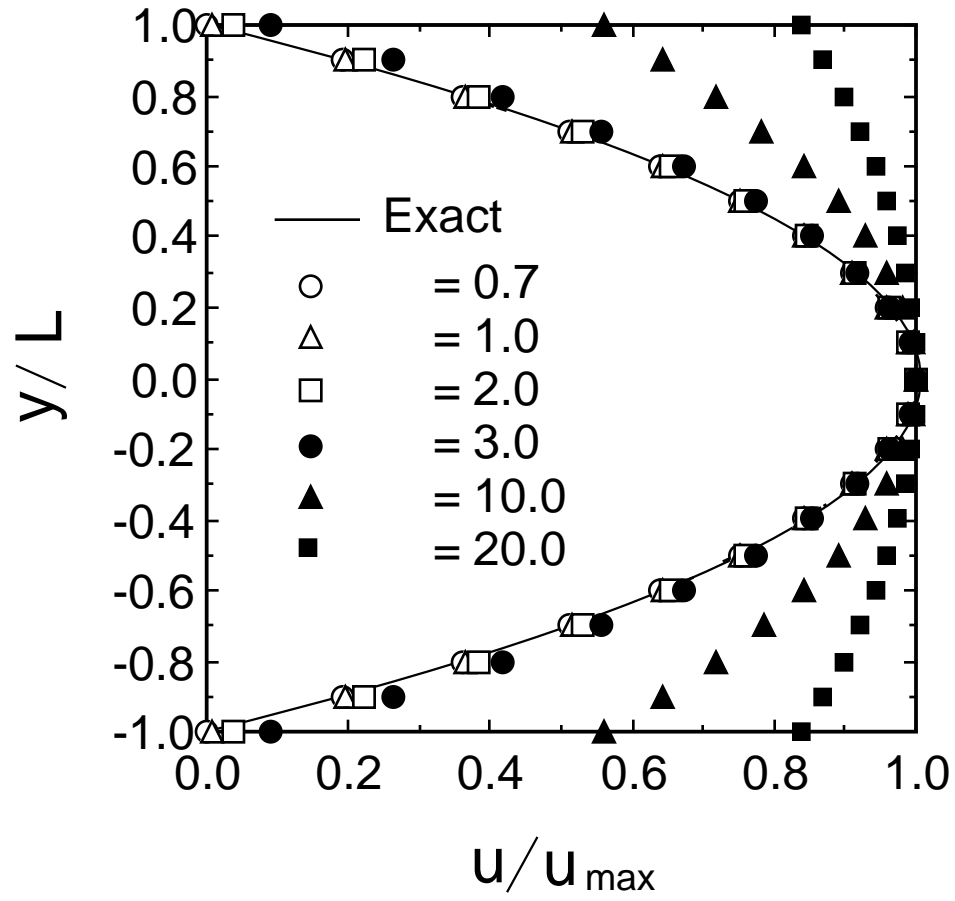velocity model at the wall.

T.Inamuro, M.Yoshino, and F.Ogino

Fig. 2. Calculated velocity profiles for Poiseuille
flow with the present boundary condition
for various values of   .

T.Inamuro, M.Yoshino, and F.Ogino

Fig. 3. Counter slip velocity u′versus single relaxation
        time in the calculations with the present bound-
        ary bounary condition.

T.Inamuro, M.Yoshino, and F.Ogino

Fig. 4. Calculated velocity profiles for Poiseuille flow with the bounce-back boundary condition for various values of .

T.Inamuro, M.Yoshino, and F.Ogino
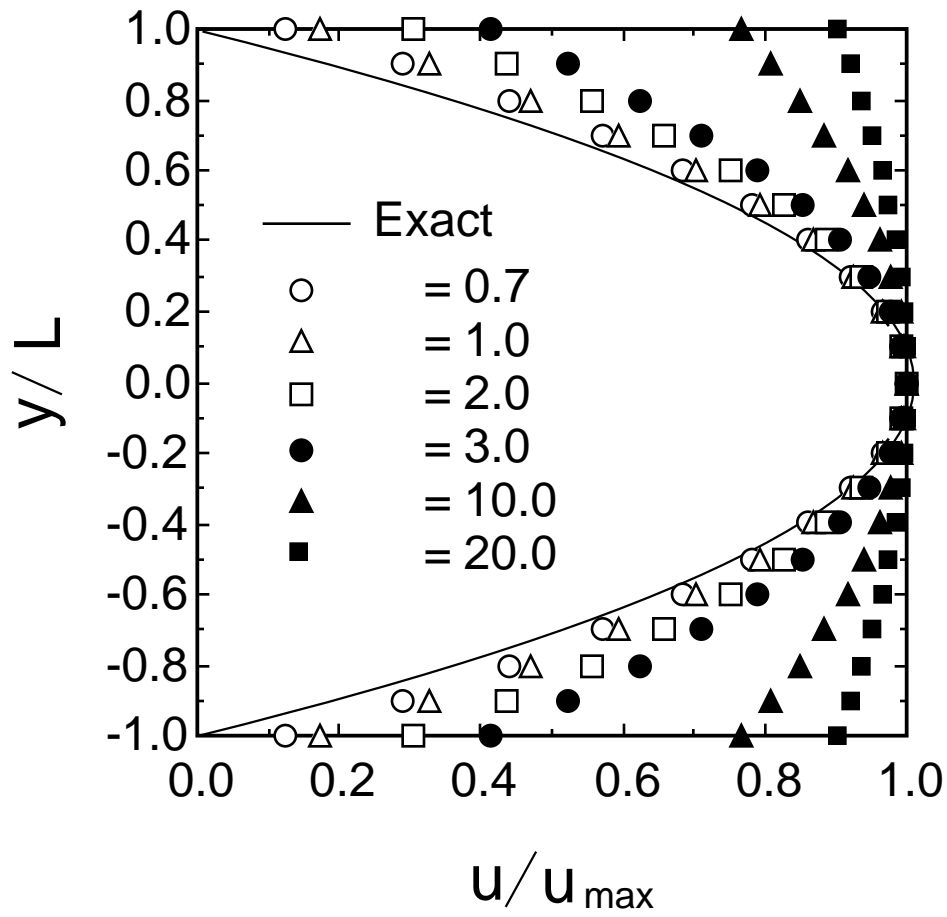
Fig. 5. Calculated velocity profiles for Poiseuille flow under the condition with $u' = 0$ in the present boundary condition for various values of .
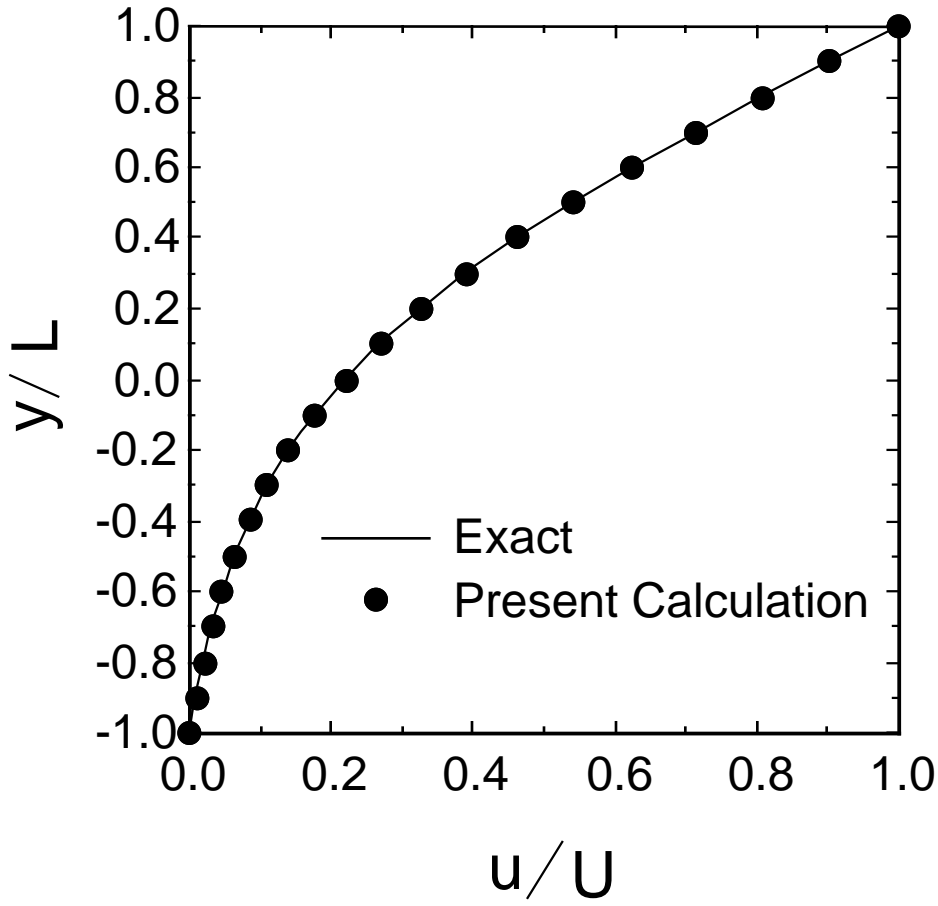
Fig. 6. Calculated velocity profiles for Couette flow at 200 time steps with 21 nodes between the walls and with = 1.
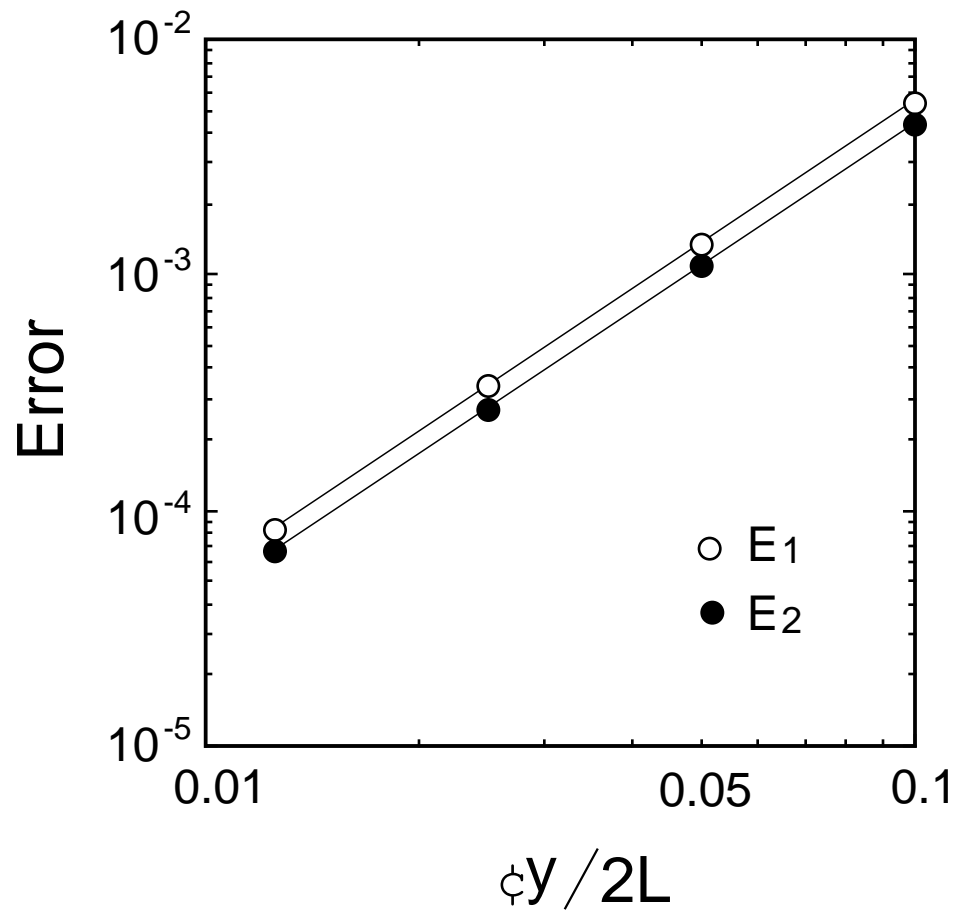
T.Inamuro, M.Yoshino, and F.Ogino

Fig. 7. Error norms for Couette flow calculations with
11, 21, 41, and 81 nodes between the walls.

T.Inamuro, M.Yoshino, and F.Ogino